

Linear and Circular Dichroism in the Double Photoionization of Helium

K. Soejima,¹ A. Danjo,¹ K. Okuno,² and A. Yagishita³

¹Graduate School of Science and Technology, Niigata University, Niigata-shi 950-21, Japan

²Department of Physics, Tokyo Metropolitan University, Hachioji-shi 192-03, Japan

³Photon Factory, Institute of Materials Structure Science, KEK, Tsukuba-shi 305, Japan

(Received 17 November 1998)

Energy- and angle-resolved triply differential cross sections have been measured in the double photoionization of helium under equal and unequal energy sharing conditions using right- and left-elliptically polarized photons. Linear dichroism in these cross sections has been observed under the equal energy sharing. For the unequal energy sharing a *pure* circular polarization effect has been deduced by eliminating the linear polarization contribution.

PACS numbers: 32.80.Fb, 33.55.Ad

The double photoionization of a helium atom occurs through a direct process due to electron correlations. Therefore, it provides the ideal test for theoretical understanding of three-body breakup in the double photoionization, if the energy- and angle-resolved triply differential cross section $d^3\sigma/d\Omega_1 d\Omega_2 d\varepsilon_1$ (TDCS) is examined. In spite of this importance, experimental investigations on the TDCS have been possible only since 1993 [1] because of experimental difficulties. Because of the lack of an available light source for circular polarization, the experimental studies of direct double photoionization processes advanced with linearly polarized light [1–3]. Although Berakdar and Klar [4] and Berakdar *et al.* [5] predicted that circular dichroism should be observed in the double photoionization of the helium atom with circularly polarized light, the first experimental evidence for the circular dichroism was reported very recently by Viefhaus *et al.* [6]. They showed the dichroism on energy sharing between the ejected electrons at three relative emission angles. However, the dichroism in the TDCS patterns between the electrons, which is very sensitive to the electron correlations, is not explored except for the most recent work of Mergel *et al.* [7]. They pointed out that the discrepancy between their experimental and theoretical results was substantial for more asymmetric energy sharing cases. In this Letter, we report the experimental results for the TDCS of the double photoionization in helium under equal and unequal energy sharing conditions and compare them with theory.

The experiment was performed at the helical undulator [8] beam line BL-28A equipped with the constant deviation monochromator [9] of the Photon Factory in Tsukuba. The photon energy of 88 eV was selected. The experimental apparatus, which had been previously discussed in more detail [10], consists of an electron-electron coincidence circuit. One electron spectrometer to detect electron e_1 is fixed ($\theta_1 = 90^\circ$, $\phi_1 = -90^\circ$ relative to the plane of the storage ring) within the plane perpendicular to the incoming photon beam Z -axis, and the other spectrometer to detect electron e_2 can be rotated ($\theta_2 = 90^\circ$, ϕ_2 variable) within this plane around the Z axis. The azimuthal angle

$\phi_{1,2}$ is measured counterclockwise from the storage ring plane as seen by an observer facing the photon beam.

Because the experimental data refer to incident light with specific polarization properties, the partial polarization of the incident light should be taken into account to express the measured TDCS. Introducing four contributions TDCS_X and TDCS_Y, which refer to linear polarization along the X and Y axis, and TDCS_R and TDCS_L, which refer to right and left circular polarization, the measured TDCS can be written as the incoherent sum of these four contributions [11]. One has

$$\begin{aligned} \text{TDCS} = & \frac{1}{2} (\text{TDCS}_X + \text{TDCS}_Y) \\ & + \frac{S_1}{2} (\text{TDCS}_X - \text{TDCS}_Y) \\ & + \frac{S_3}{2} (\text{TDCS}_R - \text{TDCS}_L), \end{aligned} \quad (1)$$

where S_1 and S_3 are the Stokes parameters describing the degree of linear and circular polarization, respectively. Kimura *et al.* [12] measured the Stokes parameters of monochromatized undulator radiation at BL-28A. They tuned the first harmonic of the undulator radiation to 97 eV, and obtained the following results; for the standard mode, $S_1 = -0.2$, $S_2 = 0$, and $S_3 = +0.95$ in the frame tilted by $\lambda = +134^\circ \pm 2^\circ$ relative to the plane of the storage ring; and, for the left-handed mode, $S_1 = +0.2$, $S_2 = 0$, and $S_3 = -0.95$ in the frame tilted by $\lambda = +44^\circ \pm 2^\circ$. The polarization parameters were not measured in the course of the present experiment, in which the photon energy was tuned to 88 eV. But we can reasonably assume the same Stokes parameters as Kimura *et al.* [12], because the degree of circular polarization at the first harmonic is independent on the undulator gap according to the calculation of Kitamura *et al.* [8].

In order to analyze the measured TDCS, we can apply the parametrization derived by Malegat *et al.* [13] to our experimental condition. If we define the X axis along $\lambda = +45^\circ$, the Y axis along $\lambda = +135^\circ$, and the mutual angle $\phi = \phi_2 - \phi_1$ ($\phi_1 = -135^\circ$) of electrons e_2 and

e_1 , the measured TDCS is parametrized as

$$\begin{aligned} \text{TDCS} = & \{(1 + \cos\phi) |M_g|^2 + (1 - \cos\phi) |M_u|^2\} \\ & + S_1 \sin\phi \{(1 - \cos\phi) |M_u|^2 - (1 + \cos\phi) |M_g|^2 - 2 \cos\phi \text{Re}(M_g M_u^*)\} - S_3 \sin\phi \{2 \text{Im}(M_u M_g^*)\}. \end{aligned} \quad (2)$$

The two complex amplitudes M_g and M_u , which describe the dynamical effects in the double photoionization, are unknown functions of kinetic energies ε_1 and ε_2 and of the mutual angle ϕ . But the M_g and M_u are symmetric and antisymmetric in the interchange of $\varepsilon_1 \leftrightarrow \varepsilon_2$, respectively; $M_g(\varepsilon_1, \varepsilon_2; \phi) = M_g(\varepsilon_2, \varepsilon_1; \phi)$ and $M_u(\varepsilon_1, \varepsilon_2; \phi) = -M_u(\varepsilon_2, \varepsilon_1; \phi)$.

Our experimental results for the ${}^{\text{eq}}\text{TDCS}(S_1 = -0.2)$ and the ${}^{\text{eq}}\text{TDCS}(S_1 = +0.2)$ are shown in Figs. 1(a) and 1(b) with the best fitted curves, respectively. The fitting procedure is described below. These data were measured under the equal energy sharing condition of $\varepsilon_1 = \varepsilon_2 = 4.5$ eV. In this special case, the ${}^{\text{eq}}M_u$ goes to zero, and the ${}^{\text{eq}}\text{TDCS}$ s are independent on S_3 . From Eq. (2), one can obtain the expression of the ${}^{\text{eq}}\text{TDCS}$:

$${}^{\text{eq}}\text{TDCS} = (1 + \cos\phi)(1 - S_1 \sin\phi) |{}^{\text{eq}}M_g|^2. \quad (3)$$

The ${}^{\text{eq}}\text{TDCS}$ has been studied by many authors under different experimental conditions [1–3,14,15], and often the $|{}^{\text{eq}}M_g|^2 \approx \exp[-4 \ln 2(180^\circ - \phi)^2 / \Gamma^2]$. According

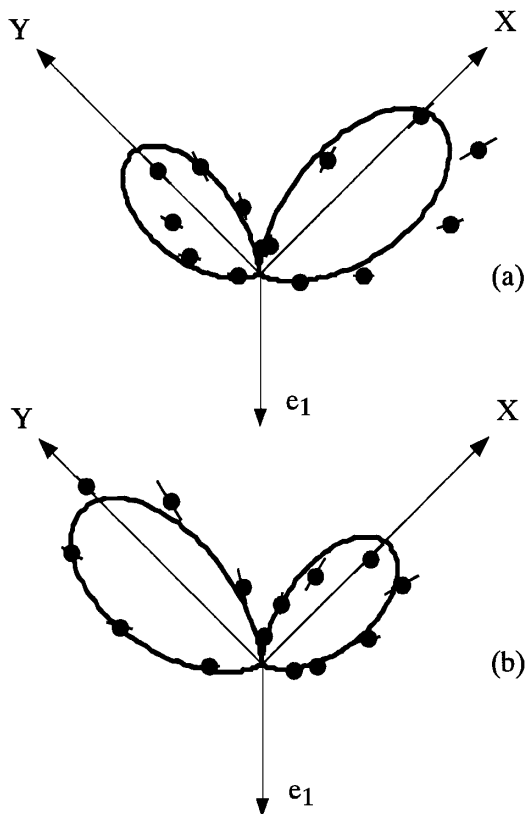


FIG. 1. Polar spots of ${}^{\text{eq}}\text{TDCS}$ under the equal energy sharing condition of $\varepsilon_1 = \varepsilon_2 = 4.5$ eV for $S_1 = -0.20$, $S_3 = +0.95$ (a) and $S_1 = +0.20$, $S_3 = -0.95$ (b). The intensities of true coincident signal are shown with error bars. The full curves present the best fitted curves using Eq. (3) (see text).

to this approximation, a least-squares fit of the ${}^{\text{eq}}\text{TDCS}$ to the experimental data has been performed using Γ and the overall size of the ${}^{\text{eq}}\text{TDCS}$ as free parameters. Then $\Gamma = 85^\circ$, and the best fitted curves in Figs. 1(a) and 1(b) have been obtained. In Fig. 1(b), one can notice a difference between the experimental data and the best fitted curve. This small difference may be due to the small change of the major axis of the polarization ellipse from $\lambda = +135^\circ$ in the course of these measurements. However, it is noted that the present result on the full width at half maximum Γ is consistent with previous observations [1–3,14,15]. Here, the comparison of Figs. 1(a) with 1(b) is emphasized. The difference between these two figures can be attributed to the only sign of S_1 , as seen from Eq. (3). The difference on the sign of S_1 , i.e., the difference for two orthogonal linear polarizations, may be called *linear dichroism* in the TDCS.

The ${}^{\text{un}}\text{TDCS}(S_1 = -0.2, S_3 = +0.95)$ and ${}^{\text{un}}\text{TDCS}(S_1 = +0.2, S_3 = -0.95)$ measured under the unequal energy sharing conditions of $\varepsilon_1 = 1$ eV and $\varepsilon_2 = 8$ eV are displayed in Figs. 2(a) and 2(b) with the best fitted curves and theoretical results [16], respectively. The fitting procedure is described below. The overall feature of our TDCSs is reproduced fairly well by the convergent close-coupling method calculations of Kheifets and Bray [16], in contrast to the substantial discrepancy point out by Kheifets and Bray [17], who compared their theoretical results with the measurements of Mergel *et al.* [7] investigated at 99 eV photon energy.

In the unequal energy sharing case, the ${}^{\text{un}}\text{TDCS}$ is expressed by the Stokes parameters of S_1 and S_3 , and the dynamical factors of ${}^{\text{un}}M_g$ and ${}^{\text{un}}M_u$ as can be seen in Eq. (2). Fortunately, it has turned out that our polarization properties enable us to perform the numerical analysis of our data. That is, when we switch the positive $S_3 = +0.95$ to the negative $S_3 = -0.95$, the negative $S_1 = -0.2$ changes to the positive $S_1 = +0.2$. Therefore, if we make the sum of the ${}^{\text{un}}\text{TDCS}(S_1 = -0.2, S_3 = +0.95)$ and ${}^{\text{un}}\text{TDCS}(S_1 = +0.2, S_3 = -0.95)$, we obtain the ${}^{\text{un}}\text{TDCS}(\text{sum})$ that is expressed by only the first term of Eq. (2):

$$\begin{aligned} {}^{\text{un}}\text{TDCS}(\text{sum}) = & 2 \times \{(1 + \cos\phi) |{}^{\text{un}}M_g|^2 \\ & + (1 - \cos\phi) |{}^{\text{un}}M_u|^2\}. \end{aligned} \quad (4)$$

The ${}^{\text{un}}\text{TDCS}(\text{sum})$ is shown in Fig. 2(c). In contrast to the equal energy sharing case, at $\phi = 180^\circ$ the ${}^{\text{un}}\text{TDCS}(\text{sum})$ has the appreciable intensity due to the contribution of $|{}^{\text{un}}M_u|^2$; $4 \times |{}^{\text{un}}M_u(1 \text{ eV}, 8 \text{ eV}, 180^\circ)|^2$. Then, the $|{}^{\text{un}}M_u|^2$ as well as the $|{}^{\text{un}}M_g|^2$ should be taken into account properly. Based on the theoretical results of Maulbetsch and Briggs [18] and Kazansky

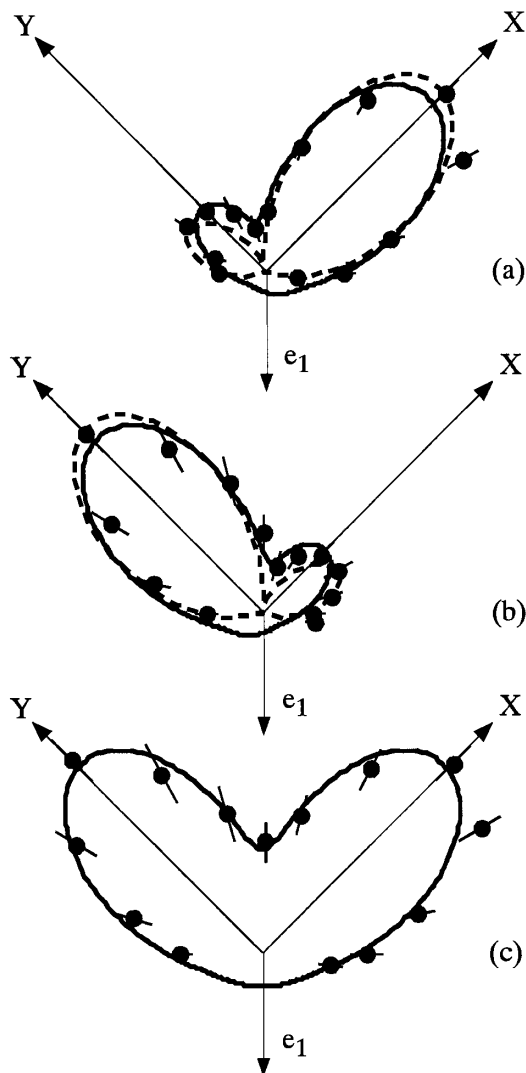


FIG. 2. Polar plots of $^{\text{un}}\text{TDCS}$ under the unequal energy sharing condition of $\varepsilon_1 = 1$ eV and $\varepsilon_2 = 8$ eV. (a) $S_1 = -0.20$, $S_3 = +0.95$; (b) $S_1 = +0.20$, $S_3 = -0.95$; and (c) sum of (a) and (b). Experimental data are shown with error bars. The full curves present the best fitted curves using Eq. (2) for (a) and (b), and Eq. (4) for (c) (see text). The dashed curves in (a) and (b) present theoretical results of Kheifets and Bray [16]. Both the experimental and theoretical results are arbitrarily scaled for comparison.

and Ostrovsky [19], the $|^{\text{un}}M_g|^2$ is approximated by the Gaussian function as stated above and a constant term A_0 :

$$|^{\text{un}}M_g|^2 = A_0 + A_1 \exp[-4 \ln 2 (180^\circ - \phi)^2 / \Gamma^2]. \quad (5)$$

For the $|^{\text{un}}M_u|^2$ function, the partial wave l expansion formula derived by Malegat *et al.* [13] is applicable. As noted in Ref. [13], it must be understood as an expansion over the configurations $l(l-1)$ of the electronic pairs which contribute to the final state. If the l_{max} is truncated by 3, the $|^{\text{un}}M_u|^2$ function is described by

$$|^{\text{un}}M_u|^2 = B_0 + B_1 \cos \phi + B_2 \cos^2 \phi + B_3 \cos^3 \phi + B_4 \cos^4 \phi, \quad (6)$$

where the coefficients of B_i are the function of ε_1 and ε_2 . A least squares fit of the $^{\text{un}}\text{TDCS}(\text{sum})$ to the experimental data has been performed using Γ , A_i , and B_i as free parameters. The best fitted curve is shown in Fig. 2(c). Figure 3(a) shows the $|^{\text{un}}M_g|^2$ and $|^{\text{un}}M_u|^2$ determined by the fitting procedure. The $|^{\text{un}}M_u|^2$ is much smaller than the $|^{\text{un}}M_g|^2$, and the ratio of the maximum of the $|^{\text{un}}M_u|^2$ to that of $|^{\text{un}}M_g|^2$ is ca. 1/30. To support the present analysis being reasonable, it is noted that this result on the ratio of $|^{\text{un}}M_u|^2 / |^{\text{un}}M_g|^2$ is consistent with the theoretical by Kazansky and Ostrovsky [19].

By introducing the phases δ_g and δ_u for the complex amplitudes of $^{\text{un}}M_g$ and $^{\text{un}}M_u$, $\text{Re}(^{\text{un}}M_g ^{\text{un}}M_u^*)$ in Eq. (2) is written as $|^{\text{un}}M_g|^2 |^{\text{un}}M_u|^2 \cos[-(\delta_u - \delta_g)]$, and $\text{Im}(^{\text{un}}M_u ^{\text{un}}M_g^*)$ is $|^{\text{un}}M_g|^2 |^{\text{un}}M_u|^2 \sin(\delta_u - \delta_g)$. Then we can parametrize the $^{\text{un}}\text{TDCS}(S_1 = -0.2, S_3 = +0.95)$ and $^{\text{un}}\text{TDCS}(S_1 = +0.2, S_3 = -0.95)$ by the phase difference $(\delta_u - \delta_g)$, since the $|^{\text{un}}M_g|^2$ and $|^{\text{un}}M_u|^2$ have been determined as shown in Fig. 3(a). A least-squares fit of the $^{\text{un}}\text{TDCS}(S_1 = -0.2, S_3 = +0.95)$ and $^{\text{un}}\text{TDCS}(S_1 = +0.2, S_3 = -0.95)$ expressed by Eqs. (2), (5), and (6) to the experimental data sets has been performed using $(\delta_u - \delta_g)$ as only one free parameter, here the values of Γ , A_i and B_i ($\Gamma = 78.7^\circ$, $A_0 = 4.28 \times 10^{-2}$, $A_1 = 3.64$, $B_0 = 0.107$, $B_1 = 9.82 \times 10^{-3}$, $B_2 = 9.44 \times 10^{-3}$, $B_3 \approx 0$, $B_4 \approx 0$ in relative scale) have been fixed. The best fitted curves corresponding to $(\delta_u - \delta_g) = +199^\circ$ are shown in Figs. 2(a) and 2(b). As can be seen in Fig. 2, the fitting results are satisfactory. Be aware that not only the contribution from the circular polarization but also the contribution from the linear polarization is taken into account, although the absolute value of S_1 is much smaller than that of S_3 in the present situation. To demonstrate how the polarization properties of the incident light influence the measured $^{\text{un}}\text{TDCS}(S_1 = -0.2, S_3 = +0.95)$, the contributions from the first term of Eq. (2), from

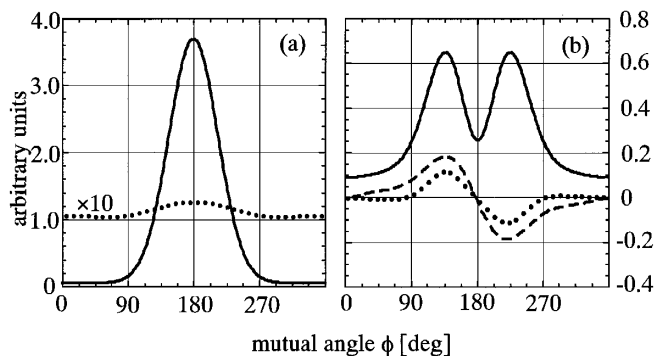


FIG. 3. (a) Full and dotted curves present the dynamical factors of $|^{\text{un}}M_g|^2$ and $|^{\text{un}}M_u|^2 \times 10$, respectively, which have been extracted from the experimental data by the fitting procedure. (b) The contributions from the first (full curve), the second (dotted curve), and the third (dashed curve) terms of Eq. (2) for $S_1 = -0.20$ and $S_3 = +0.95$. For the case of $S_1 = +0.20$ and $S_3 = -0.95$, the signs of the contributions from the second and the third terms are inverted.

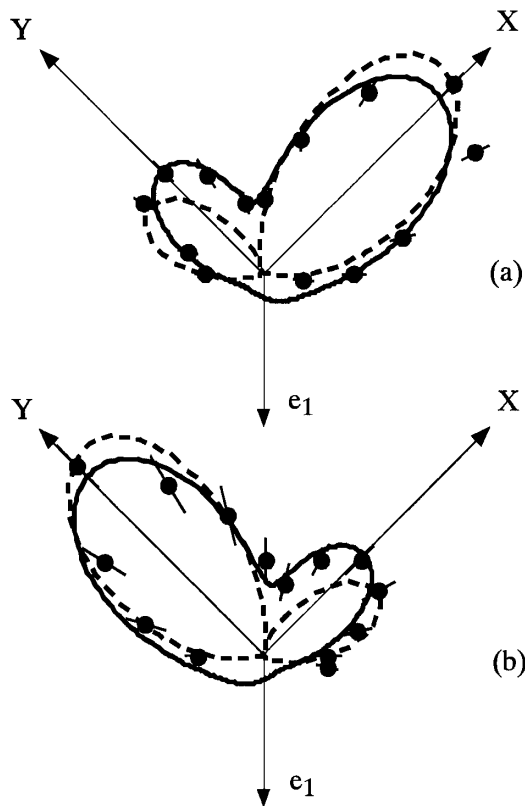


FIG. 4. Polar plots of ${}^{\text{un}}\text{TDCS}(R)$ and ${}^{\text{un}}\text{TDCS}(L)$ deduced by subtracting the S_1 part from the ${}^{\text{un}}\text{TDCS}$. (a) ${}^{\text{un}}\text{TDCS}(R)$ for $S_3 = +0.95$; and (b) ${}^{\text{un}}\text{TDCS}(L)$ for $S_3 = -0.95$. Experimental data are shown with error bars. The full curves express the best fitted curve. The dashed curves present theoretical results of Kheifets and Bray [16] for $S_1 = 0$ and $S_3 = +0.95$. Both the experimental and theoretical results are arbitrarily scaled for comparison.

the second term of Eq. (2), and from the third term of Eq. (2) are indicated separately in Fig. 3(b). Surprisingly, the contribution from the second term has the comparable magnitude to that from the third term. As the sign of S_1 is opposite to that of S_3 , the difference between ${}^{\text{un}}\text{TDCS}(S_1 = -0.2, S_3 = +0.95)$ and ${}^{\text{un}}\text{TDCS}(S_1 = +0.2, S_3 = -0.95)$ cannot give so-called *circular dichroism* in TDCS. It can be said that mirror symmetry between Figs. 2(a) and 2(b) with respect to $\phi = 180^\circ$ is an accidental result, because the mirror symmetry between the major axes of the polarization ellipses for $S_1 = \pm 0.2$ and $S_3 = \mp 0.95$, which we cannot control, with respect to $\phi = 180^\circ$ was caused accidentally.

As can be understood from Fig. 3(b), we can construct the ${}^{\text{un}}\text{TDCS}(R)$ and ${}^{\text{un}}\text{TDCS}(L)$ including solely the dependence on the S_3 by subtracting the S_1 part from the ${}^{\text{un}}\text{TDCS}(S_1 = -0.2, S_3 = +0.95)$ and ${}^{\text{un}}\text{TDCS}(S_1 = +0.2, S_3 = -0.95)$, respectively. Figures 4(a) and 4(b) show the ${}^{\text{un}}\text{TDCS}(R)$ for $S_3 = +0.95$ and ${}^{\text{un}}\text{TDCS}(L)$ for $S_3 = -0.95$. The difference between Figs. 4(a) and 4(b), which have the mirror symmetry for

kinematical reason, is the “pure” *circular dichroism* in TDCS. And it is evidently caused by the interference term of $\text{Im}({}^{\text{un}}M_u {}^{\text{un}}M_g^*)$. Eliminating the S_1 contribution, the large ratio of maxima at the two lobes of the TDCS pattern is considerably reduced in comparison with the raw data of Fig. 2. The theoretical results of Kheifets and Bray [16] are shown in Fig. 4 for comparison. Agreement between our results and their calculations is fairly well in the similar manner to the comparison of Fig. 2. As to the origin of the burdened minimum in our data, the small change of the tilted angle of the major axes from $\lambda = +45^\circ$ and $\lambda = +135^\circ$ in the course of these measurements is considered except for the influence of the solid angles $\pm 12^\circ$ of our analyzers.

By taking the polarization properties of the incident light into account and by applying the parametrization of Malegat *et al.* [13], we have succeeded in, for the first time, deriving the symmetric amplitude $|M_g|$, antisymmetric amplitude $|M_u|$, and phase difference $(\delta_u - \delta_g)$ between them from our experimental data. Because these parameters give the full description for the dynamical effects in double photoionization continuum, the present approach opens a door toward the further step to elucidate the general Coulombic three-body problem.

-
- [1] O. Schwarzkopf, B. Krässig, J. Elimiger, and V. Schmidt, *Phys. Rev. Lett.* **70**, 3008 (1993).
 - [2] A. Huetz *et al.*, *J. Phys. B* **27**, L13 (1994).
 - [3] P. Lablanquie *et al.*, *Phys. Rev. Lett.* **74**, 2192 (1995).
 - [4] J. Berakdar and H. Klar, *Phys. Rev. Lett.* **69**, 1175 (1992).
 - [5] J. Berakdar, H. Klar, A. Huetz, and P. Selles, *J. Phys. B* **26**, 1463 (1993).
 - [6] J. Viefhaus *et al.*, *Phys. Rev. Lett.* **77**, 3975 (1996).
 - [7] V. Mergel *et al.*, *Phys. Rev. Lett.* **80**, 5301 (1998).
 - [8] H. Kitamura, *Insertion Device Handbook 1990 Photon Factory*, edited by H. Kitamura, KEK Report 89-24 (National Laboratory for High Energy Physics, Tsukuba, Japan, 1990).
 - [9] Y. Kagoshima *et al.*, *Rev. Sci. Instrum.* **63**, 1289 (1992).
 - [10] K. Soejima *et al.*, *J. Korean Phys. Soc.* **32**, 368 (1998).
 - [11] S.J. Schaphorst *et al.*, *J. Electron Spectrosc.* **76**, 229 (1995).
 - [12] H. Kimura *et al.*, *Rev. Sci. Instrum.* **66**, 1920 (1995).
 - [13] L. Malegat, P. Selles, and A. Huetz, *J. Phys. B* **30**, 251 (1997).
 - [14] A. Huetz *et al.*, *The Physics of Electronic and Atomic Collisions*, edited by L.J. Dubé *et al.* (AIP, New York, 1995), p. 139.
 - [15] L. Malegat *et al.*, *J. Phys. B* **30**, 263 (1997).
 - [16] A. S. Kheifets and I. Bray (private communication).
 - [17] A. S. Kheifets and I. Bray, *Phys. Rev. Lett.* **81**, 4588 (1998).
 - [18] F. Maulbetsch and J. S. Briggs, *J. Phys. B* **27**, 4095 (1994).
 - [19] A. K. Kazansky and V. N. Ostrovsky, *Phys. Rev. A* **51**, 3698 (1995).